Electronic Supplementary Material (ESI) for Nanoscale.

Unravelling the Reactivity of Metastable Molybdenum Carbide Nanoclusters in C-H Bond Activation of Methane, Ethane and Ethylene

Sonit Balyan[a,b], Shikha Saini[c], Tuhin S. Khan[d]*, K. K. Pant[b], Puneet Gupta[e]*, Saswata Bhattacharya[c]* and M. Ali Haider[a]*

[a] Renewable Energy and Chemicals Lab, Department of Chemical Engineering, Indian Institute of Technology Delhi, Hauz Khas, New Delhi, India

[b] Catalytic Reaction Engineering Lab, Department of Chemical Engineering, Indian Institute of Technology Delhi, Hauz Khas, New Delhi, India

[c] Department of Physics, Indian Institute of Technology Delhi, Hauz Khas, New Delhi, India

[d] Light Stock Processing Division, CSIR-Indian Institute of Petroleum, Dehradun, 248005, India

[e] Computational Catalysis Center, Department of Chemistry, Indian Institute of Technology Roorkee, Roorkee, Uttarakhand, India

Corresponding authors email addresses: tuhins.khan@iip.res.in, puneet.gupta@cy.iitr.ac.in, saswata@physics.iitd.ac.in, haider@iitd.ac.in

Table S1. Radial functions as considered for tight setting of basis set for C, and Mo in cGA.

Minimal	[He] + 2s 2p	[Kr] + 5s 4p 4d
Tier 1	H(2p,1.7)	H(4f,8.4)
	H(3d,6.0)	H(3d,2.8)
	H(2s,4.9)	I(5p)
		H(5g,12.0)
		I(5s)
Tier 2	H(4f,9.8)	H(4f,12.4)
	H(3p,5.2)	H(3d,3.3)
	H(3s,4.3)	H(6h,17.2)
	H(3d,6.2)	H(4f,7.6)
		H(3p,3.0) H(1s,0.65)

Here, the first line (minimal) represents the free-atom radial functions (noble-gas configuration of the core and quantum numbers of the additional valence radial functions). "H(nl,z)" is the hydrogen-like basis function for the bare Coulomb potential (z/r) that includes its radial and angular momentum quantum numbers, *n* and *l*. I(nl) is a n,l radial function of a free ion of species Mo.

Table S2. Geometry of Mo_2C_6, Nanocluster **1.**

Bond length, Å		**Bond angle, degree**		**Atom**	X	Y	Z
$Mo^{(1)}$-$Mo^{(2)}$	2.65	$C^{(1)}$-$Mo^{(1)}$-$C^{(1)}$	89	Mo	-0.0029	0.4573	0.1725
$Mo^{(1)}$-$C^{(1)}$	1.88	$Mo^{(1)}$-$Mo^{(2)}$-$C^{(1)}$	45	Mo	1.7880	0.5994	2.2251
$Mo^{(1)}$-$C^{(11)}$	1.94	$C^{(11)}$-$Mo^{(1)}$-$C^{(1)}$	103	C	1.0825	1.8174	0.9356
$C^{(11)}$-$C^{(111)}$, $C^{(111)}$-$C^{(111)}$	1.31	$Mo^{(1)}$-$Mo^{(2)}$-$C^{(11)}$	99	C	0.7790	-0.7828	1.3819
				C	-1.6235	0.8237	1.2068
				C	-1.5691	1.0342	2.4819
				C	-0.8530	1.1268	3.5666
				C	0.4472	0.9827	3.5739

Table S3. Geometry of Mo_2C_6, Nanocluster **2.**

Bond length, Å		**Bond angle, degree**		**Atom**	X	Y	Z
$Mo^{(1)}$-$Mo^{(2)}$	2.58	$C^{(1)}$-$Mo^{(1)}$-$C^{(111)}$, $Mo^{(1)}$-$Mo^{(2)}$-$C^{(V1)}$	90	Mo	1.2723	-0.2657	-0.1394
$Mo^{(1)}$-$C^{(1)}$	1.95	$C^{(1)}$-$Mo^{(1)}$-$C^{(111)}$	96	C	1.4393	1.7211	-0.3956
$Mo^{(1)}$-$C^{(11)}$	2.00	$C^{(1V)}$-$Mo^{(1)}$-$Mo^{(2)}$	91	C	0.4965	-1.0265	1.48709
$Mo^{(1)}$-$C^{(111)}$	2.14	$C^{(1)}$-$Mo^{(2)}$-$Mo^{(1)}$	49	C	-1.9567	-0.4760	-0.0885
$Mo^{(1)}$-$C^{(1V)}$	1.92	$C^{(1)}$-$Mo^{(1)}$-$Mo^{(2)}$	46	Mo	-0.8295	0.2640	1.2689
$Mo^{(2)}$-$C^{(1)}$	1.86	$C^{(111)}$-$Mo^{(2)}$-$Mo^{(1)}$	54	C	0.1933	-1.0140	-1.5425
$Mo^{(2)}$-$C^{(111)}$	2.01	$C^{(111)}$-$Mo^{(1)}$-$Mo^{(2)}$	50	C	-0.9478	-0.8110	-0.9015
$Mo^{(2)}$-$C^{(V1)}$	1.90	$C^{(111)}$-$Mo^{(1)}$-$C^{(11)}$, $C^{(111)}$-$Mo^{(1)}$-$C^{(11)}$	37	C	0.3325	1.6083	0.3116
$C^{(11)}$-$C^{(111)}$	1.31	$C^{(11)}$-$Mo^{(1)}$-$C^{(1)}$,	121				
$C^{(1V)}$-$C^{(V)}$	1.32	$C^{(1V)}$-$Mo^{(1)}$-$C^{(2)}$	110				
$C^{(V)}$-$C^{(V1)}$	1.34	$C^{(1V)}$-$Mo^{(1)}$-$C^{(111)}$, $C^{(1V)}$-$Mo^{(2)}$-$C^{(11)}$	104				
		$C^{(V1)}$-$Mo^{(2)}$-$C^{(111)}$, $C^{(1V)}$-$Mo^{(1)}$-$C^{(111)}$	105				
		$Mo^{(2)}$-$Mo^{(1)}$-$C^{(11)}$	86				

Table S4. Geometry of Mo_2C_6, Nanocluster **3.**

Bond length, Å		**Bond angle, degree**		**Atom**	X	Y	Z
$Mo^{(1)}$-$Mo^{(2)}$	2.37	$C^{(1)}$-$Mo^{(1)}$-$C^{(1)}$	92	Mo	-0.7815	-0.7815	0.1086
$Mo^{(1)}$-$C^{(1)}$	1.90	$C^{(11)}$-$Mo^{(1)}$-$C^{(1)}$	120	Mo	0.8679	-1.3208	1.3181
$Mo^{(1)}$-$C^{(11)}$	2.10	$Mo^{(1)}$-$Mo^{(2)}$-$C^{(1)}$	52	C	-0.8813	1.8560	0.8366
$C^{(11)}$-$C^{(111)}$	1.27	$Mo^{(1)}$-$Mo^{(2)}$-$C^{(11)}$	110	C	1.7396	-0.0507	2.7587
$C^{(111)}$-$C^{(1V)}$	1.35			C	0.0337	1.5653	1.6655
				C	0.9766	0.8794	2.3569
				C	-1.0141	-1.5815	1.3015
				C	1.3015	-0.8175	-0.5141

Table S5. Geometry of Mo_2C_6, Nanocluster **4.**

Bond length, Å		**Bond angle, degree**		**Atom**	X	Y	Z
$Mo^{(1)}$-$Mo^{(2)}$	2.68	$C^{(1)}$-$Mo^{(1)}$-$Mo^{(2)}$	119	Mo	1.5689	-1.4269	0.8050
$Mo^{(1)}$-$C^{(1)}$	1.97	$C^{(1)}$-$Mo^{(1)}$-$C^{(111')}$	120	Mo	-0.8851	-1.1393	-0.2518
$Mo^{(1)}$-$C^{(11)}$	2.05	$C^{(1)}$-$Mo^{(1)}$-$C^{(11)}$	39	C	-2.3817	-0.6356	0.9382
$Mo^{(1)}$-$C^{(111)}$	2.01	$C^{(1)}$-$Mo^{(1)}$-$C^{(111)}$	78	C	-0.2424	-1.8352	1.5238
$Mo^{(1)}$-$C^{(111')}$	2.0	$C^{(11)}$-$Mo^{(1)}$-$C^{(111)}$	40	C	1.6544	0.5949	0.5155
$C^{(1)}$-$C^{(11)}$	1.34	$C^{(11)}$-$Mo^{(1)}$-$C^{(111')}$	107	C	-1.4647	-1.2483	1.7056
$C^{(11)}$-$C^{(111)}$	1.37	$C^{(11)}$-$Mo^{(1)}$-$Mo^{(2)}$	83	C	0.7322	0.0201	-0.3155
		$C^{(111)}$-$Mo^{(1)}$-$C^{(111')}$	88	C	2.5203	0.1798	1.4551
		$C^{(111)}$-$Mo^{(1)}$-$Mo^{(2)}$	48				

Table S6. Geometry of Mo_2C_6, Nanocluster **5.**

Bond length, Å		**Bond angle, degree**		**Atom**	X	Y	Z
$Mo^{(1)}$-$Mo^{(11)}$	2.24	$C^{(1)}$-$Mo^{(1)}$-$C^{(11)}$	37	Mo	-0.5856	1.1176	-0.9092
$Mo^{(1)}$-$C^{(1)}$	2.08	$C^{(1)}$-$Mo^{(1)}$-$C^{(111)}$	133	C	1.3777	1.4868	-1.2440
$Mo^{(1)}$-$C^{(11)}$	2.04	$C^{(1)}$-$Mo^{(1)}$-$C^{(1V)}$	114	C	1.4229	-0.1130	0.8581
$Mo^{(1)}$-$C^{(111)}$	2.10	$C^{(1)}$-$Mo^{(1)}$-$Mo^{(2)}$	57	C	-2.1169	-1.4947	-0.1321
$Mo^{(1)}$-$C^{(1V)}$	2.25	$C^{(1)}$-$Mo^{(2)}$-$Mo^{(1)}$	58	Mo	-0.8441	-0.2389	0.8573
$Mo^{(2)}$-$C^{(1)}$	2.06	$C^{(11)}$-$Mo^{(1)}$-$C^{(111)}$	123	C	-1.6955	-0.6188	-1.0131
$Mo^{(2)}$-$C^{(V)}$	2.23	$C^{(11)}$-$Mo^{(1)}$-$C^{(1V)}$	130	C	1.5042	0.7215	-0.2036
$Mo^{(2)}$-$C^{(V1)}$	2.02	$C^{(11)}$-$Mo^{(1)}$-$Mo^{(2)}$	94	C	0.9372	-0.8604	1.7867
$C^{(1)}$-$C^{(11)}$	1.31	$C^{(111)}$-$Mo^{(1)}$-$C^{(1V)}$	34				
$C^{(111)}$-$C^{(1V)}$	1.29	$C^{(111)}$-$Mo^{(1)}$-$Mo^{(2)}$	116				
$C^{(1V)}$-$C^{(V)}$	1.35	$C^{(1V)}$-$Mo^{(1)}$-$Mo^{(2)}$	82				
$C^{(V)}$-$C^{(V1)}$	1.30	$C^{(V)}$-$Mo^{(2)}$-$Mo^{(1)}$	75				
		$C^{(V)}$-$Mo^{(2)}$-$C^{(1)}$	111				
		$C^{(V)}$-$Mo^{(2)}$-$C^{(V1)}$	35				
		$C^{(V1)}$-$Mo^{(2)}$-$Mo^{(1)}$	110				
		$C^{(V1)}$-$Mo^{(2)}$-$C^{(1)}$	131				

Table S7. Comparison of activation energy of methane C-H bond activation over different Mo_2C_6 nanocluster.

Cluster	Activation energy, kJ/mol
Nanocluster **1**	127.4
Nanocluster **2**	67.7
Nanocluster **3**	94.6
Nanocluster **4**	125
Nanocluster **5**	90.7

Table S8. Comparison of activation energies calculated for methane dehydrogenation over different sites on the metastable Mo_2C_6 nanocluster **2**.

Activation site	Activation energy, kJ/mol
$Mo^{(1)}$-$C^{(1)}$	67.7
$Mo^{(1)}$-$C^{(11)}$	92.3
$Mo^{(2)}$-$C^{(1)}$	120.1
$Mo^{(2)}$-$C^{(111)}$	144.1

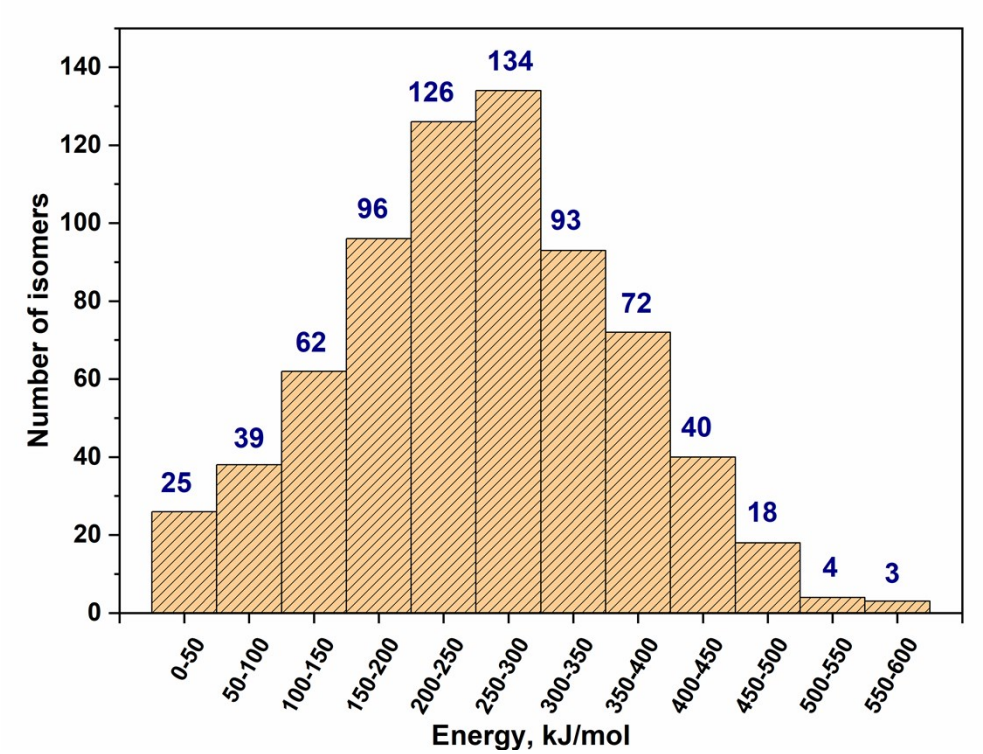

Figure S1. Histogram showing the number of Mo_2C_6 structures scanned in the cGA search in the energy span of 600 kJ/mol starting with the lowest energy structure used as reference.

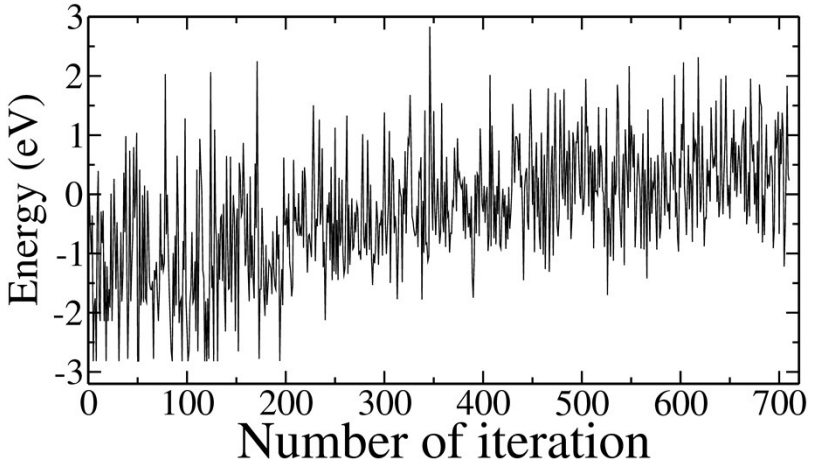

Figure S2. Variations in the energy of the nanoclusters in iterative search on the potential energy surface in cGA.

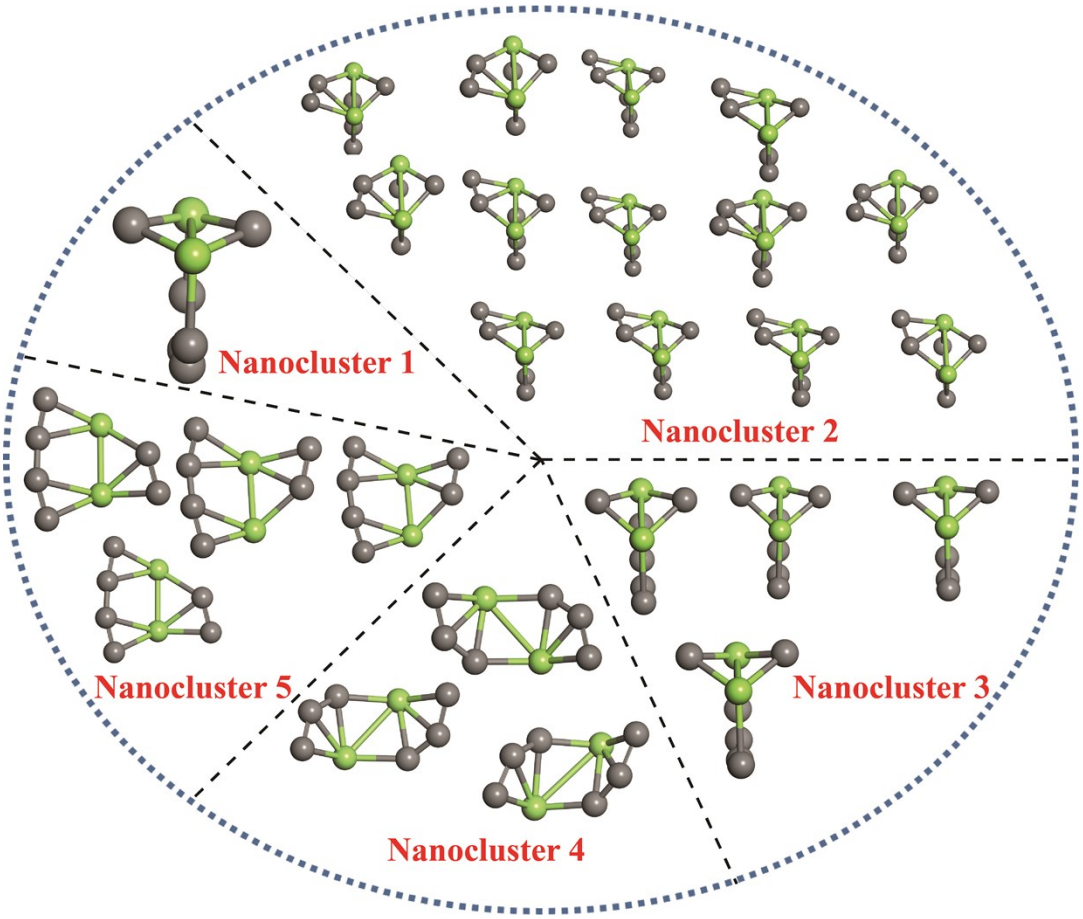

Figure S3. Isomers of structures of Mo_2C_6 nanoclusters obtained from the cGA search in energy span window of 50 kJ/mol with respect to the reference lowest energy nanocluster.

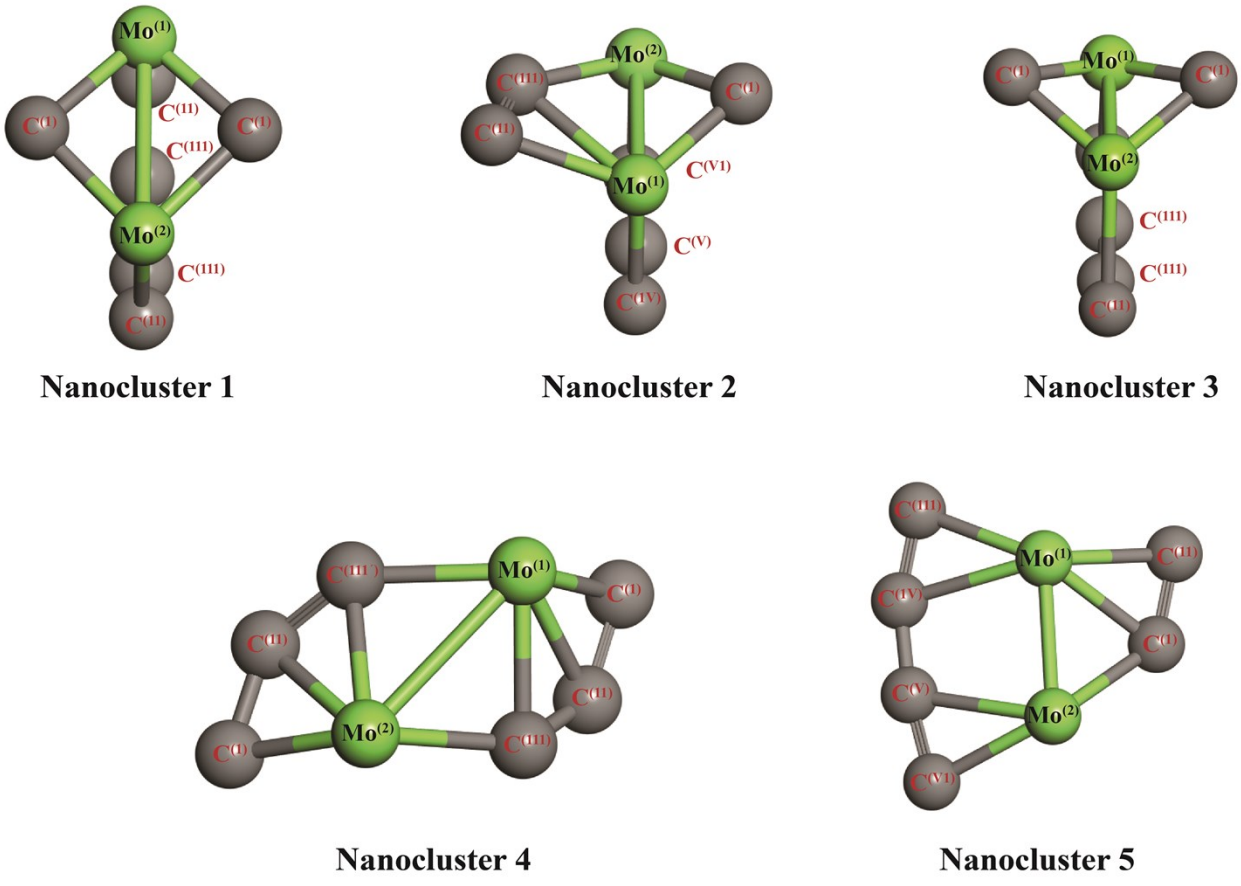

Figure S4. Structure of Mo_2C_6 nanocluster with atom numbering labels for geometries in Table S2-6.

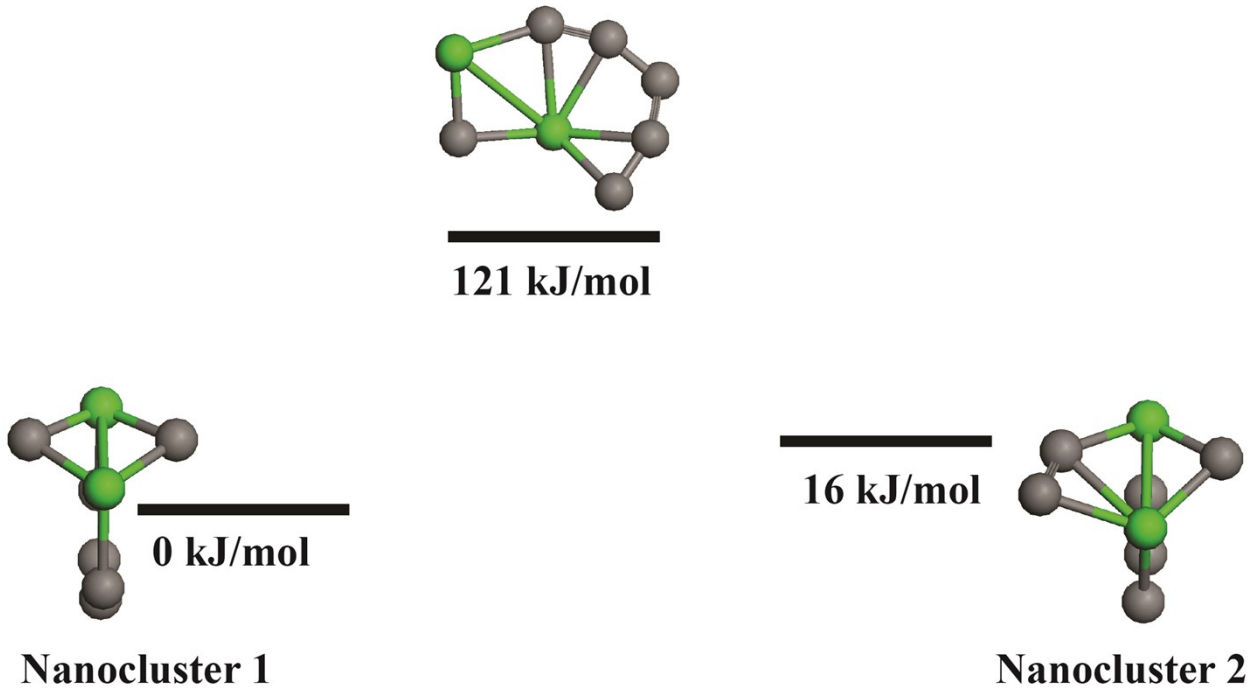

Figure S5. Energy diagram showing the fluxionality between the lowest energy (nanocluster **1**) and metastable (nanocluster **2**) forms of Mo_2C_6 via an intermediate structure.

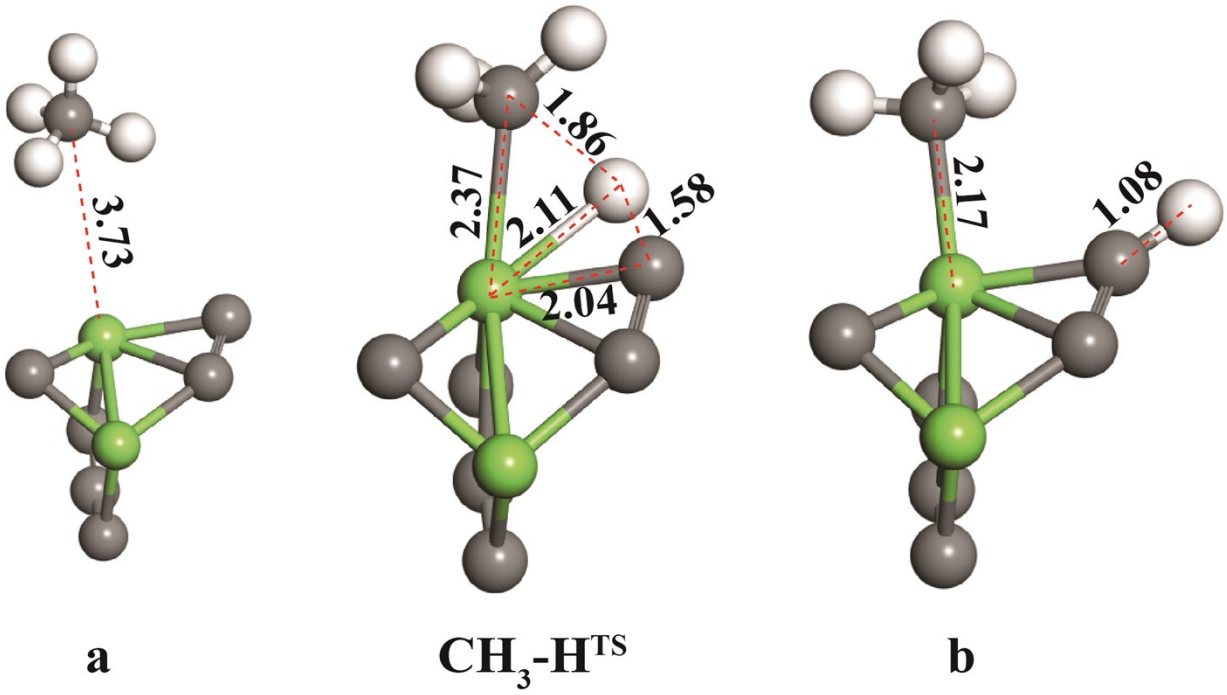

78

79 **Figure S6.** Reactant, transition and product state structures for methane dehydrogenation over

80 the $Mo^{(1)}$-$C^{(11)}$ site of nanocluster **2** (bond lengths in angstrom).

81

82

83

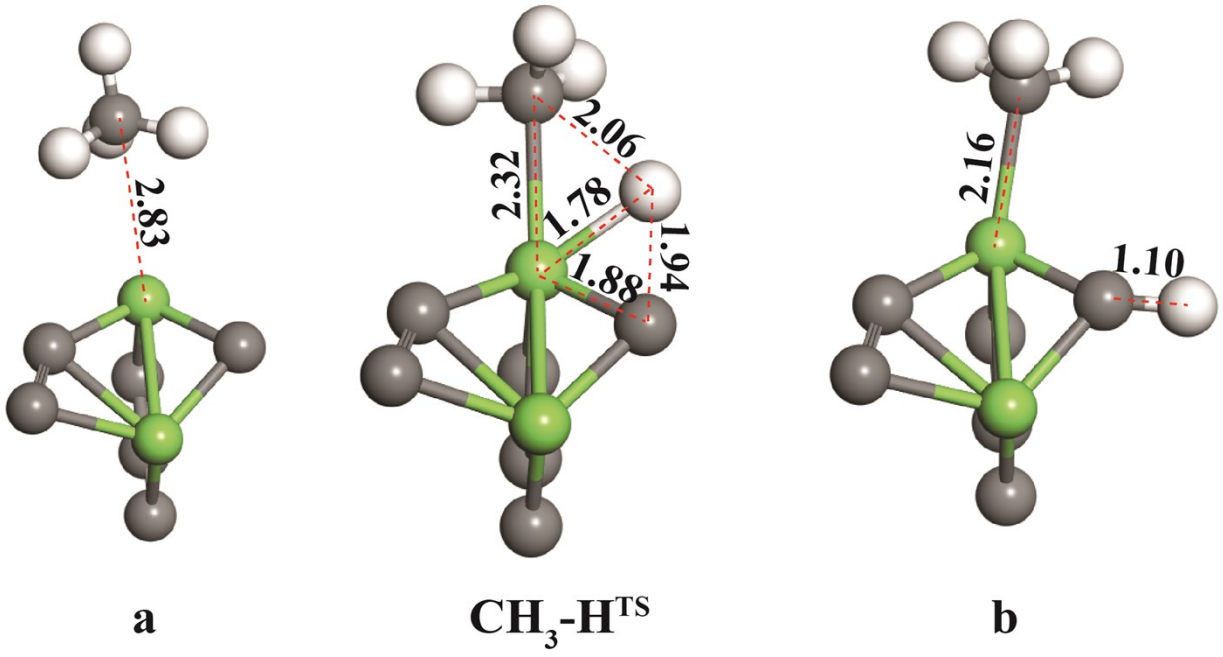

Figure S7. Reactant, transition and product state structures for methane dehydrogenation over the $Mo^{(2)}$-$C^{(1)}$ site of nanocluster **2** (bond lengths in angstrom).

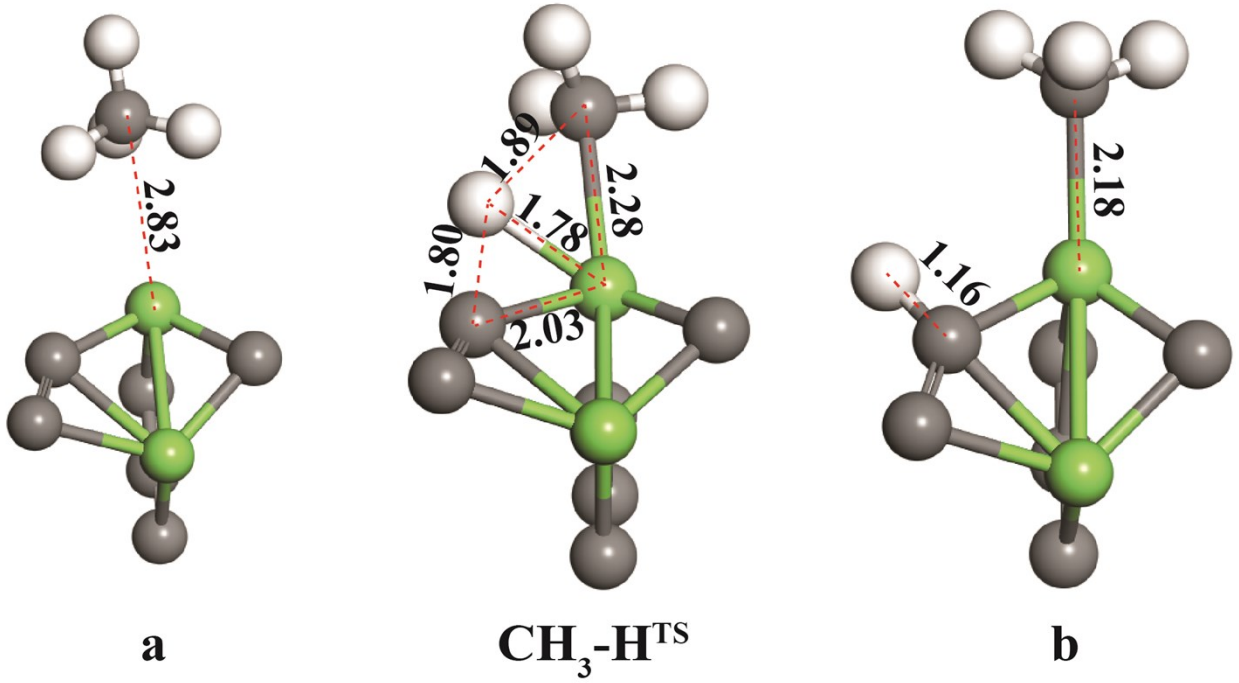

Figure S8. Reactant, transition and product state structures for methane dehydrogenation over the $Mo^{(2)}$-$C^{(111)}$ site of nanocluster **2** (bond lengths in angstrom).

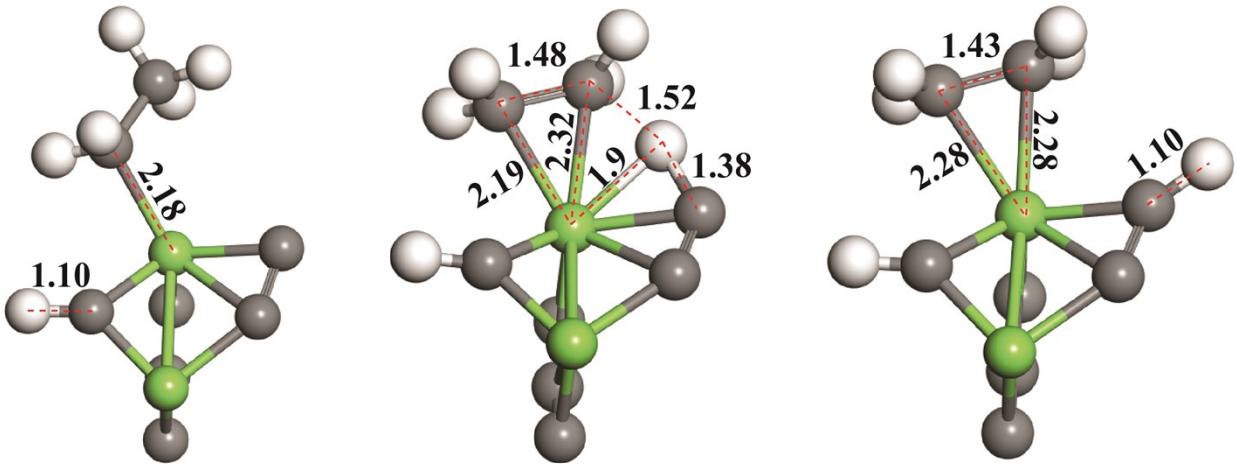

Figure S9. Geometry of reactant, transition and product state structures for $C_2H_5^*$ dehydrogenation over the $Mo^{(1)}$-$C^{(11)}$ site of nanocluster **2** (bond lengths in angstrom).

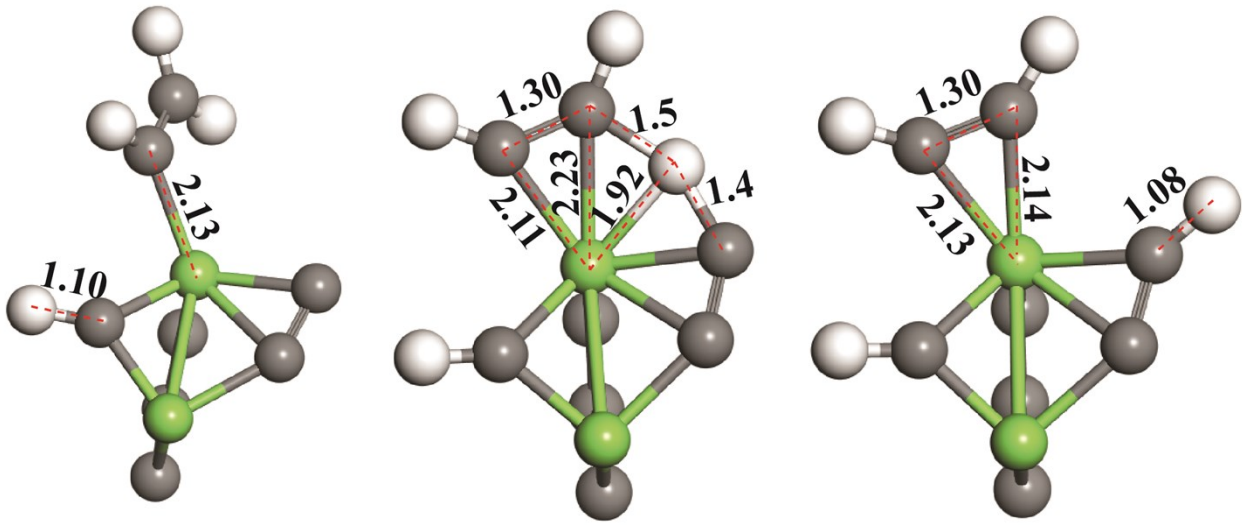

Figure S10. Geometry of reactant, transition and product state structures for $C_2H_3^*$ dehydrogenation over the $Mo^{(1)}$-$C^{(11)}$ site of nanocluster **2** (bond lengths in angstrom).

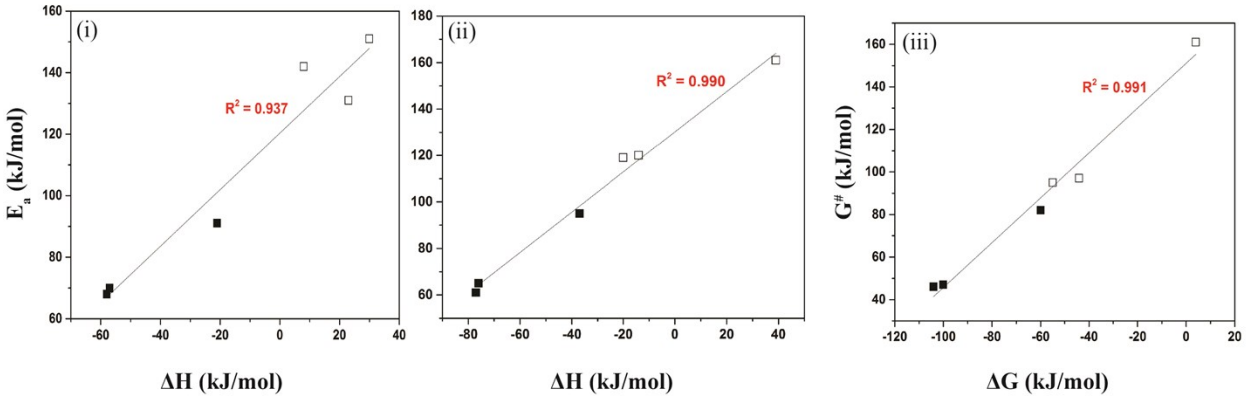

Figure S11. BEP relationships plotted for C-H activation in methane, ethane and ethylene over the lowest energy nanocluster **1** (open symbols) and metastable nanocluster **2** (filled symbol) using the (i) RPBE functional with fixed nanocluster coordinate, (ii) RPBE functional with relaxed nanocluster coordinate and (iii) B3LYP functional with relaxed nanocluster coordinate.

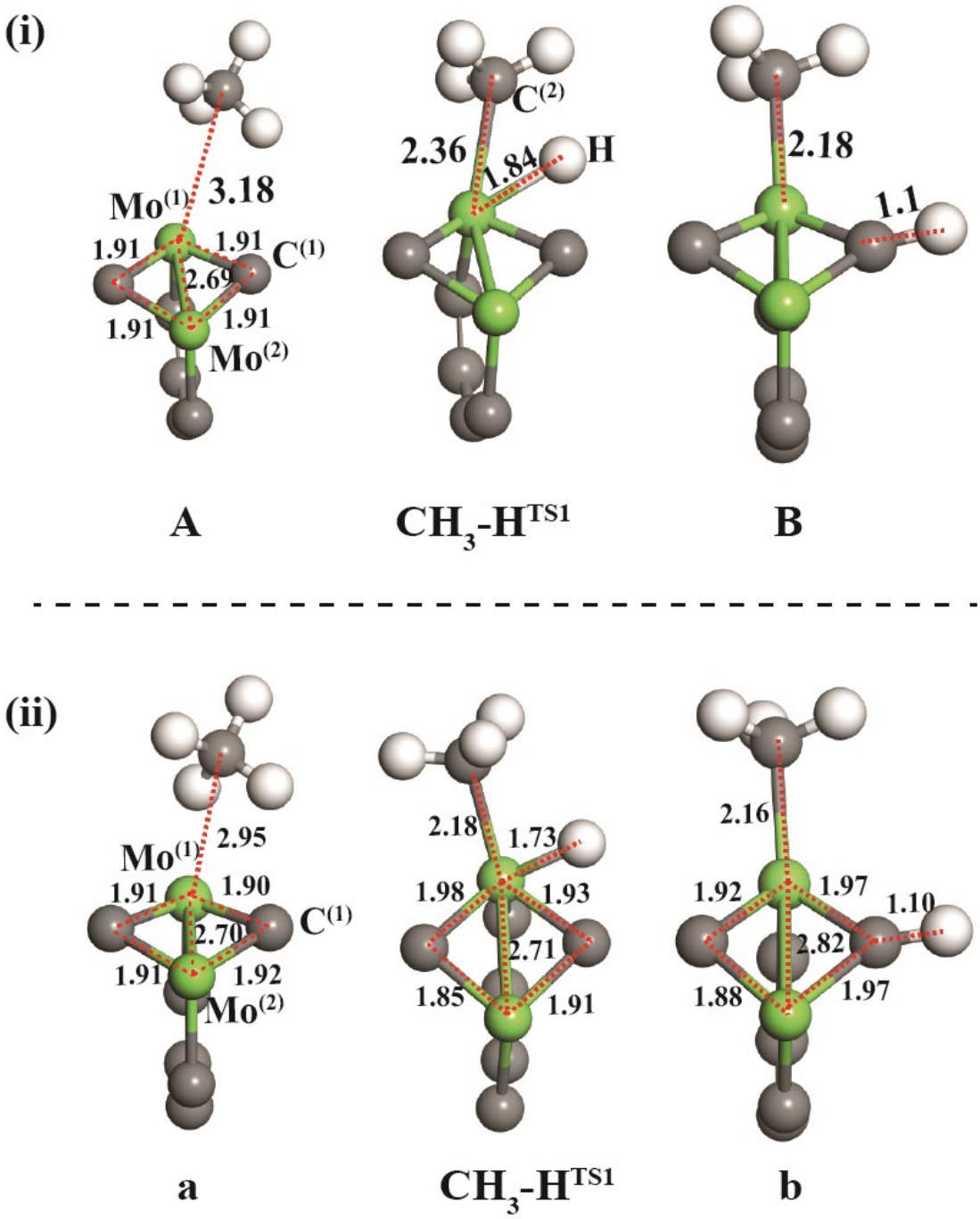

Figure S12. Reactant, transition and product state structures for methane dehydrogenation reaction over the $Mo^{(1)}$-$C^{(1)}$ site of lowest energy nanocluster **1** for (i) constrained and (ii) unconstrained structure (bond lengths are shown in angstrom).